BONDED CONCRETE OVERLAY OF ASPHALT PAVEMENTS MECHANISTIC-EMPIRICAL DESIGN GUIDE (BCOA-ME)

THEORY MANUAL

University of Pittsburgh
Department of Civil and Environmental Engineering
Pittsburgh, Pennsylvania 15261

Prepared by:
Zichang Li
Nicole Dufalla
Feng Mu
Julie M. Vandenbossche, Ph.D., P.E.

Prepared for:
FHWA Pooled Fund Project: TPF-5-165

August 2013

The bonded concrete overlay of asphalt pavements mechanistic-empirical design guide (BCOA-ME) has been developed to supply a Portland cement concrete (PCC) overlay thickness based on design inputs such as climate parameters, existing structural parameters, as well as asphalt and concrete material properties. The purpose of this theory manual is to elaborate on the process and calculations utilized in the design procedure. This manual is subdivided into four categories: traffic, temperature gradient, HMA modulus, and the fatigue analysis. Inputs will be discussed and the calculations and theory used will be presented.

1. Traffic Considerations

In this design procedure, traffic calculations are performed using the concept of 18-kip equivalent single axle loads (ESALs). The equation used for calculating design ESALs is given as:

$$ESAL_{design} = DD \times LDF \times G_f \times ESAL_{daily} \times 365 \tag{1}$$

where,

DD is the directional distribution factor and indicates the fraction of total traffic in the design direction. For one-way traffic, which is required for this procedure, the default value is 1.0.

LDF is the lane distribution factor and is adopted from AASHTO 1993 (p. II-9) as a function of the number of traffic lanes in each direction.

G_f is the traffic growth factor which is calculated using either Equation (2) or Equation (3) depending on the type of growth rate.

$ESALs_{daily}$ is the sum of daily equivalent single axle loads determined for each type of axle load given by Equation (4).

The traffic growth factor for a nonlinear growth rate is given by:

$$G_f = \frac{\left[\left(1 + G_{r,ADTT}\right)^n - 1\right]}{G_{r,ADTT}} \tag{2}$$

The traffic growth factor for a linear growth rate is given by:

$$G_f = n \times \left(1 + G_{r,ADTT} \times \frac{(n-1)}{2}\right) \tag{3}$$

where,

$G_{r,ADTT}$ is the user-inputted growth rate of average daily truck traffic (ADTT).

n is the design life, years.

The ESALs for a specific type of axle loading is estimated using:

$$ESALs_{daily} = N_R \times LEF \tag{4}$$

where,

N_R is the number of repetitions for a specific axle load per day and can be calculated from Equation (5).

LEF is the load equivalency factor and is calculated through the AASHTO relationship given in Equation (7).

$$N_R = \frac{ADTT}{1000} \times Axles\ per\ 1000\ trucks \tag{5}$$

where,

$Axles\ per\ 1000\ trucks$ information is adopted from the axle load distributions provided in the ACPA guidelines for "Design of Concrete Pavement for City Streets" (2002) and is a function of road category, the axle type, and the axle load, as shown in Table 1.

Table 1: $Axles\ per\ 1000\ trucks$ for different road categories. Source: "Design of Concrete Pavement for City Streets" (2002).

Axle load (Kips)	Axles per 1000 trucks			
	Category LR	**Category 1**	**Category 2**	**Category 3**
Single axles				
4	846.15	1693.31	0.00	0.00
6	369.97	732.28	0.00	0.00
8	283.13	483.10	233.60	0.00
10	257.60	204.96	142.70	0.00
12	103.40	124.00	116.76	182.02
14	39.07	56.11	47.76	47.73
16	20.87	38.02	23.88	31.82
18	11.57	15.81	16.61	25.15
20	0.00	4.23	6.63	16.33
22	0.00	0.96	2.60	7.85
24	0.00	0.00	1.60	5.21
26	0.00	0.00	0.07	1.78
28	0.00	0.00	0.00	0.85
30	0.00	0.00	0.00	0.45
Tandem axles				
4	15.12	31.90	0.00	0.00
8	39.21	85.59	47.01	0.00
12	48.34	139.30	91.15	0.00
16	72.69	75.02	59.25	99.34
20	64.33	57.10	45.00	85.94
24	42.24	39.18	30.74	72.54
28	38.55	68.48	44.43	121.22
32	27.82	69.59	54.76	103.63
36	14.22	4.19	38.79	56.25
40	0.00	0.00	7.76	21.31
44	0.00	0.00	1.16	8.01
48	0.00	0.00	0.00	2.91
52	0.00	0.00	0.00	1.19

LR = Light residential

ADTT is the average daily truck traffic given as:

$$ADTT = ADT \times Truck\ percent \tag{6}$$

where,

ADT is the user-inputted average daily traffic. If unavailable, ADTT can be estimated based on the typical values of ADTT for different road categories given in Table 2.

$Truck\ percent$ is the percentage of total traffic comprised of trucks. A default value of 6% is provided in the design procedure.

Table 2: ADTT given for different road categories and classifications.

Classification	**ADTT**	**Road category**
Light Residential	3	LR
Residential	10 to 50	1
Collector	50 to 500	2
Business	400 to 700	
Minor Arterial	300 to 600	
Industrial	300 to 800	3
Major Arterial	700 to 1500	

The LEF used in Equation (4) can be estimated using the following equation:

$$LEF = \left(\frac{W_x}{W_{18}}\right)^{-1} \tag{7}$$

where,

W_x is the number of 18-kip ESALs for any loading x, and $W_x = W_{18}$ for x = 18 kips. W_x is calculated using the following equation:

$$\text{Log}(W_x) = 5.908 - 4.62\log(L_x + L_2) + 3.28\log(L_2) + \frac{G_t}{\beta_x} + \frac{G_t}{\beta_{18}} \tag{8}$$

where,

L_x is the axle loading, kips.

L_2 is the weight of the axle, kips (1 for single axle and 2 for tandem axle).

β_x is a constant to reflect the current loading in kips, x. $\beta_x = \beta_{18}$ for x = 18 kips. They are given by Equations (9) and (10).

$G_t$is the growth rate and is given by Equation (11).

$$\beta_x = 1 + \frac{3.63(L_x + L_2)^{5.2}}{(h_{PCC} + 1)^{8.46} {L_2}^{3.52}} \tag{9}$$

$$\beta_{18} = 1 + \frac{1.62\ x10^7}{(h_{PCC} + 1)^{8.46}} \tag{10}$$

where,

h_{PCC} is the PCC thickness, in.

$$G_t = \log\left(\frac{4.5 - P_t}{4.5 - 1.5}\right) \tag{11}$$

where,

P_t is the pavement terminal serviceability.

2. Temperature Gradient

The temperature gradient causes the slab to curl and creates an environmental stress in addition to the stress due to traffic loading. In the available structural models for whitetopping slabs, a linear temperature gradient is required to calculate this environmental stress. Since the temperature variation through the slab is nonlinear, an accurate estimate of environmental stress is not possible with the linear temperature gradient. The effective equivalent linear temperature gradient (EELTG) is thus proposed as an input that characterizes the environmental stress.

The framework used to establish the EELTG is illustrated by Figure 1. A database was first populated to produce a number of whitetopping sites that represent all the climatic conditions in the continental United States, as shown in Figure 2. For each site shown in Figure 2, there exist multiple whitetopping projects representing different structural features, such as PCC overlay thickness, existing asphalt thickness, etc. The nonlinear temperature gradient for each project was then obtained on an hourly basis using the Enhanced Integrated Climatic Model (EICM) (Larson and Dempsey, 2003) considering different whitetopping structures. The hourly nonlinear temperature gradients were then converted to hourly equivalent linear temperature gradients (ELTGs) based on strain equivalency. Finally, the EELTG was determined as the equivalent linear temperature gradient that when applied throughout the design life results in the same fatigue damage as if the hourly linear temperature gradients were used.

Based on the database, a relationship was found statistically between the EELTG and the climatic and structural features of the PCC overlay. The relation for the EELTG is expressed separately for three different slab sizes given in Equations (12) through Equation (14). More details regarding establishing this input can be found in the Task 4 report of this project (Barman et al, 2013).

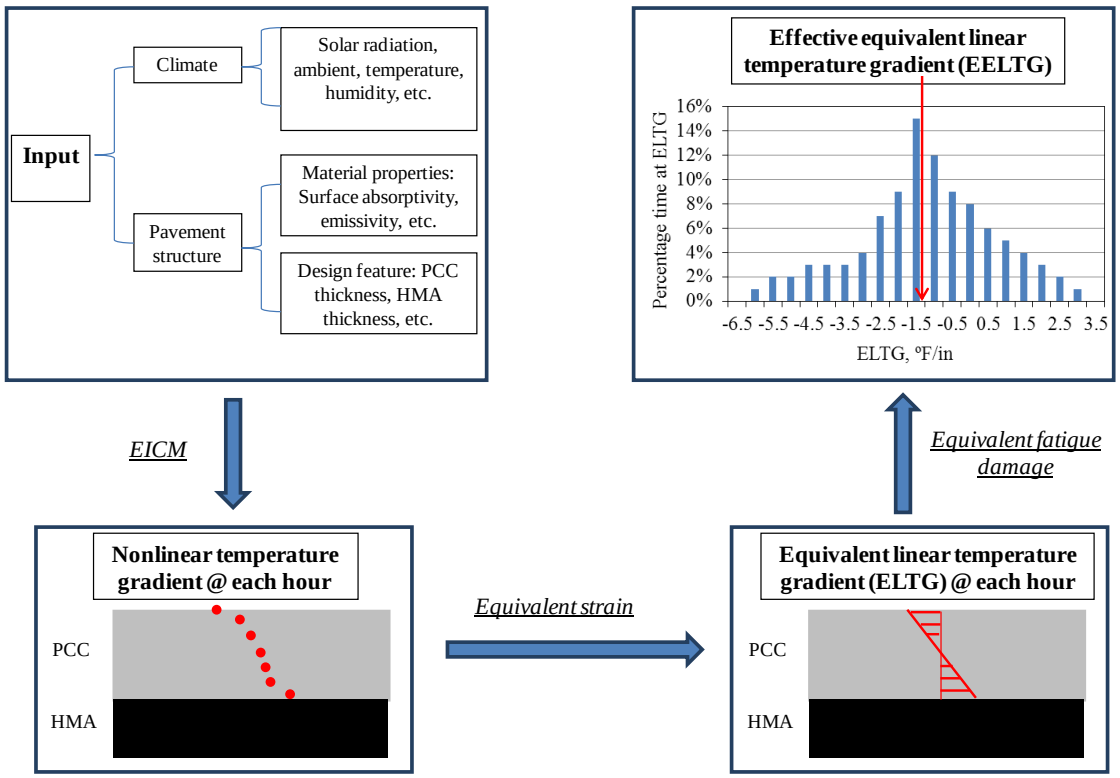

Figure 1: Flowchart to generate the effective equivalent linear temperature gradient.

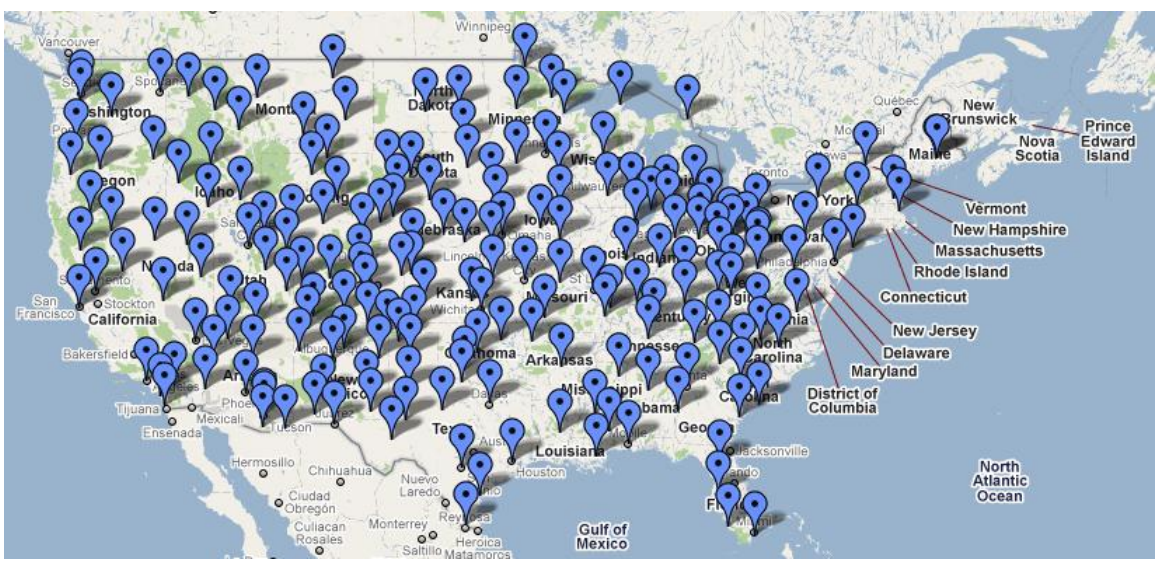

Figure 2: Whitetopping sites representing all climates of the continental United States (The background map is the Google Map of the US as of June, 2010).

2.1 Equations for the EELTG

For smaller slabs (slabs with a joint spacing ≤ 4.5 ft × 4.5 ft), the $EELTG_{small\ slabs}$ is given by:

$$EELTG_{small\ slabs} = 0.534 - 0.0015644Latitude - 0.0009853Longitude - 0.00002145Elevation - 0.0067836S_{ave} + 0.15843L - 0.202627h_{HMA} - 0.00175066M_R \quad (12)$$

For mid-size slabs (slabs with a joint spacing > 4.5 ft and ≤ 7 ft), the $EELTG_{mid-size\ slabs}$ is given by:

$$EELTG_{mid-size\ slabs} = 0.85895 + 0.0046918\ Latitude + 0.0018581\ Longitude + 0.000003625\ Elevation - 0.0082567\ S_{ave} - 0.127695\ h_{HMA} + 0.00077175\ M_R \quad (13)$$

For larger slabs which span a single lane width, the $EELTG_{large\ slabs}$ is given by:

$$EELTG_{larg\ slabs} = 2.791 + 0.011843\ Latitude + 0.00134661\ Longitude + 0.0000058\ Elevation + 0.0091791\ S_{ave} - 0.070225\ h_{HMA} + 0.0013025\ M_R - 0.45202\ h_{pcc} \quad (14)$$

where,

$EELTG$ is the effective equivalent linear temperature gradient, °F/in.

$Latitude$ is the geographical latitude of the project location, degrees

$Longitude$ is the geographical longitude of the project location, degrees

$Elevation$ is the distance of the project location above sea level, feet

S_{ave} is the annual mean percentage of sunshine, %.

L is the PCC overlay slab size, ft.

h_{HMA} is the hot mix asphalt (HMA) layer thickness, in.

h_{pcc} is the PCC overlay thickness, in.

M_R is the PCC modulus of rupture, psi.

2.2 Determination of Inputs for EELTG

The calculation of EELTG requires user-defined geographic inputs including latitude, longitude, and elevation, as well as user-defined design inputs including the PCC overlay slab size, HMA layer thickness, and the PCC modulus of rupture. Additionally, the annual mean percentage of sunshine (S_{ave}) is also required and typical values based on geographic zones are given in Figure 3.

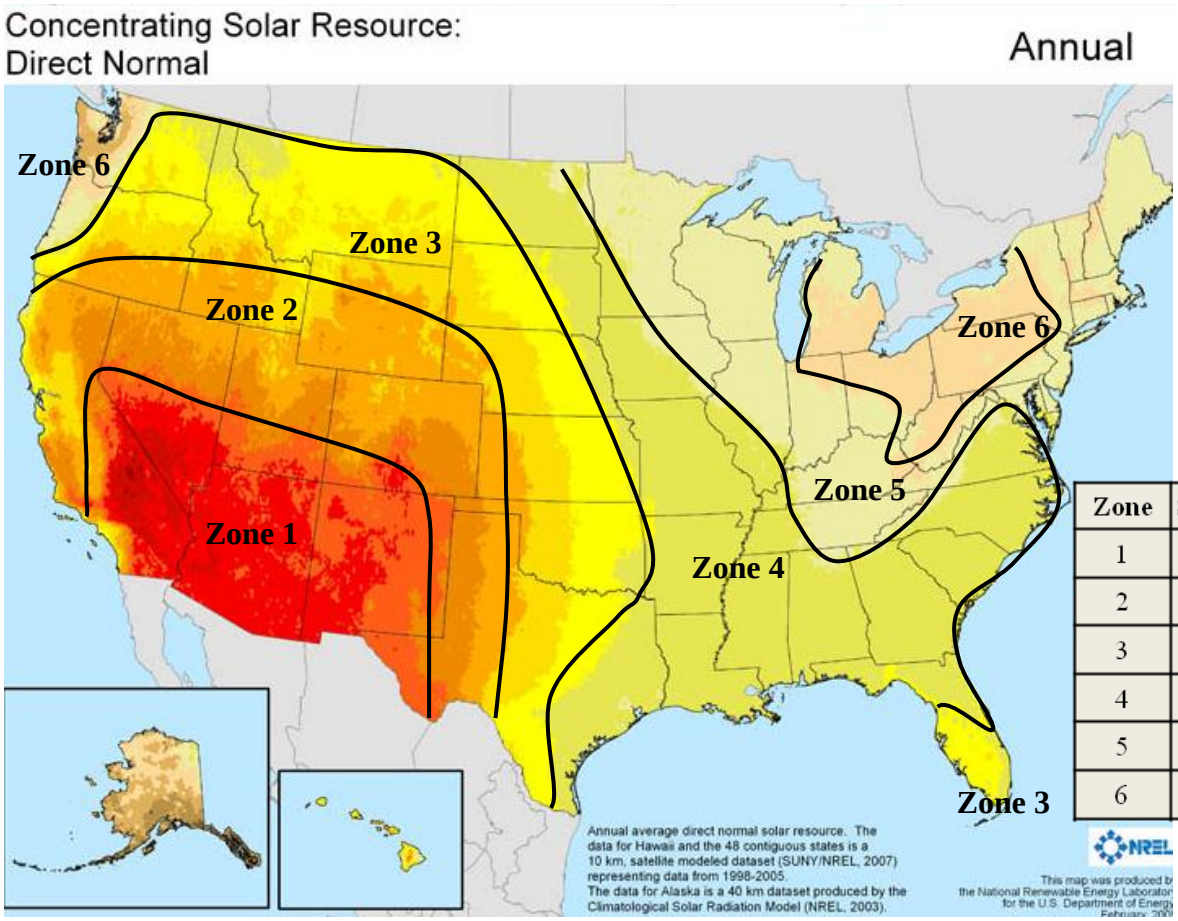

Zone	S_{ave}(%)
1	73
2	71
3	59
4	59
5	52
6	44

Figure 3: Zonal division of the US in terms of the annual mean percentage of sunshine (based on the annual concentrating solar resource map of the US in 2009, http://www.nrel.gov/gis/solar.html).

3. Characterization of the HMA Modulus

The HMA modulus changes directly with seasonal and daily temperature variations; however, in all available design procedures, a constant HMA modulus is used. This assumption predicts uniform fatigue consumption throughout the year while accounting for the increased

fatigue consumption that occurs during the summer months. In this design procedure, the HMA modulus adjustment factors are used to adjust the reference month HMA modulus that account for both the seasonal and hourly variation of the HMA modulus on the fatigue of the overlay.

An investigation was carried out to determine the factors affecting the temperature-related HMA modulus fluctuation. This investigation revealed that the time of year (season) and the geographic location of the project were the two primary factors influencing the HMA modulus fluctuation. To take seasonal temperature variations across the country into account, seven temperature regions were established based on the annual mean daily average temperature (AMDAT) map as shown in Figure 4.

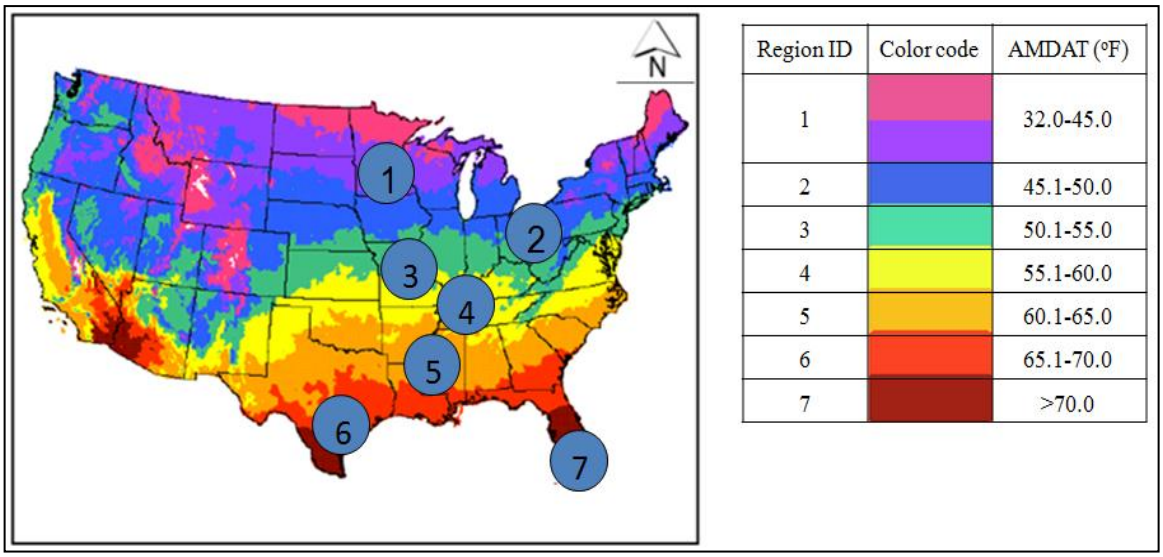

Figure 4: Regional division of the US in terms of the annual mean daily average temperature (AMDAT) (http://cdo.ncdc.noaa.gov/climaps/temp0313).

3.1 Considerations in Establishing Effective HMA Modulus Values.

The framework used to establish the HMA asphalt stiffness adjustment factor (*F*) for the seven different temperature regions is shown in Figure 5. For every weather station in each region, monthly HMA temperature is first estimated using the Enhanced Integrated Climatic Model (EICM). The same database of weather stations used for the EELTG analysis was selected as shown in Figure 2. Then, using the master curve (ARA, 2004) the HMA modulus for different temperatures was determined for each region. A uniform aggregate gradation was chosen for all regions. SHRP LTPPBIND version 3.1 (Pavement System LLC, 2005) which is a Superpave binder selection program developed for the Federal Highway Administration

(FWHA) was used to choose asphalt binder grade according to the location of the project for each zone. Then, the hourly and monthly HMA modulus for each weather station was determined using the corresponding hourly and monthly mean temperature of the region.

The fatigue accumulation using the hourly HMA modulus for a certain month is denoted as FA_h, while the fatigue accumulation using the monthly HMA modulus for the same month is FA_m. The difference between FA_h and FA_m indicates the effect of hourly HMA modulus variation and it is a function of design features and material properties. A large number of hypothetical designs are considered for the fatigue analysis. The design variables considered in the fatigue analysis can be found in Table 3.

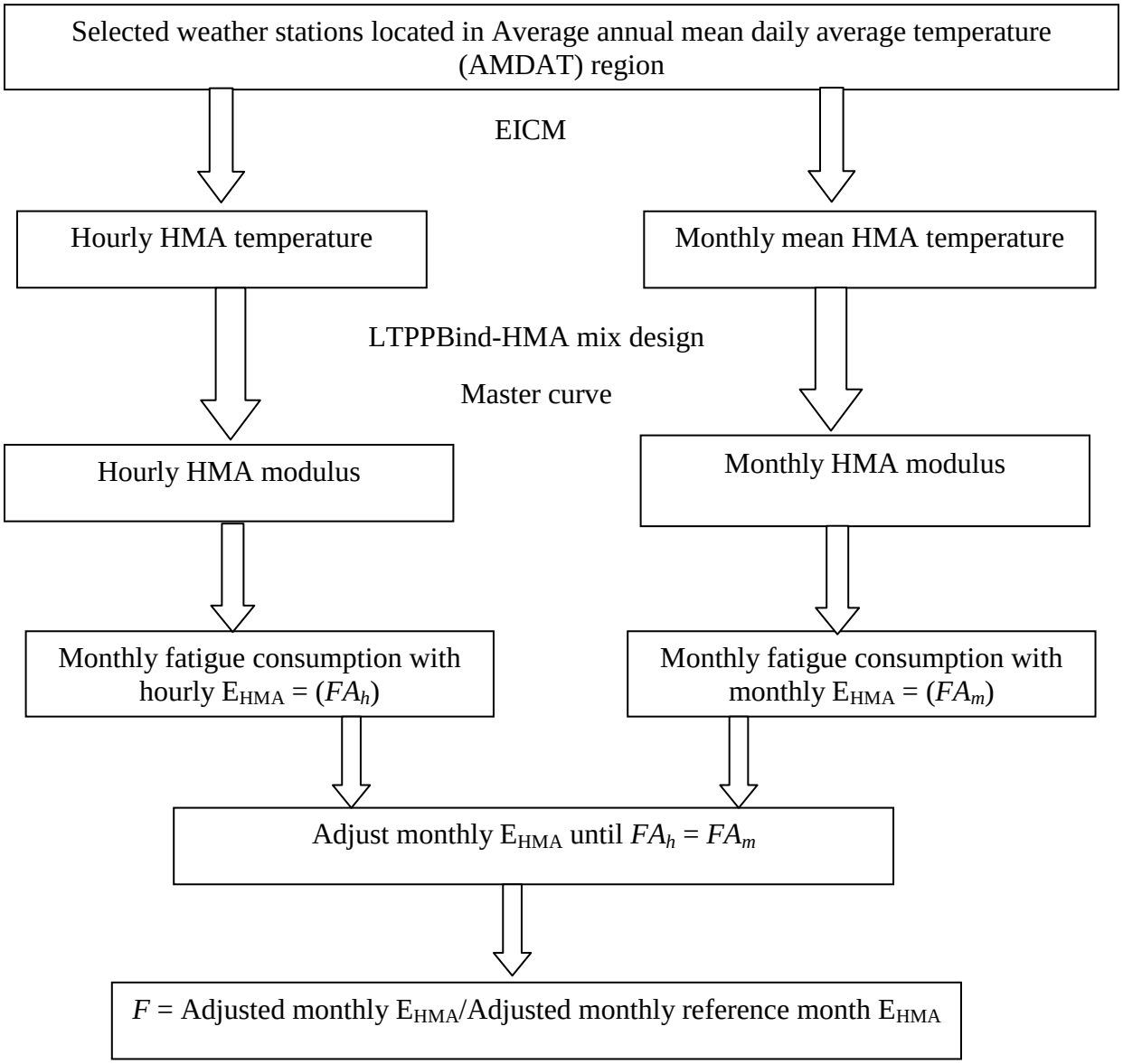

Figure 5: Framework for establishing the effective HMA modulus adjustment factor, (F).

Table 3: Whitetopping design features and material properties considered in the fatigue analysis.

Design features in the fatigue analysis			
Joint spacing	PCC layer thickness (in)	HMA layer thickness (in)	Panel size (ft ×ft)
≤4.5 ft	3 and 4	4 and 8	3 × 3 and 4 × 4
>4.5 ft ≤ 7 ft	3, 4, and 6	4 and 8	6 × 6
> 7 ft	5 and 6	4, 6, and 8	10 × 12

Material properties					
Concrete MOR (psi)	PCC modulus (10^6 psi)	Concrete CTE ($10^{-6}/^0$F)	k (pci)	Poisson's ratio of PCC	Poisson's ratio of HMA
550, 650 and 750	3.5, 4, 4.4	5	200	0.15	0.35

For each design at a certain location, there are twelve effective monthly HMA Modulus values, which were normalized to a reference month, defined as the HMA modulus adjustment factors (*F*). Regression models are then developed for *F* as a function of HMA thickness and normalized mid-depth HMA temperature, as demonstrated in Equation (15). These equations reflect the change of HMA modulus as a function of seasonable and hourly temperature variation. As shown in Figure 4, the seasonal temperature variation across the country can be subdivided into seven temperature regions according to the annual mean daily average temperature (AMDAT). Three different design methods are used based upon the slab size, resulting in three sets of values for the regression coefficients in Equation (15), and are given with R^2 values in Table 4.

$$F = C_1 + \frac{C_2}{T_{Norm}} + C_3 * h_{HMA} + C_4 * h_{PCC} \tag{15}$$

where,

F is the HMA modulus adjustment factor that accounts for seasonal variation of the HMA modulus and the effect of the hourly temperature variation on the fatigue of the overlay.

h_{HMA} is the HMA thickness, in.

T_{norm} is normalized mid-depth HMA temperature of the project location.

h_{PCC} is the PCC overlay thickness, in

Table 4: HMA modulus adjustment factor coefficients by zone.

≤ 4.5 ft × 4.5 ft joint spacing	Zone 1	Zone 2	Zone 3	Zone 4	Zone 5	Zone 6	Zone 7
C_1	-0.139	-0.246	-0.300	-0.310	-0.525	-0.654	-0.428
C_2	1.07	1.25	1.32	1.31	1.51	1.66	1.41
C_3	-0.00576	-0.00657	-0.00804	-0.00764	-0.00335	-0.00540	-0.00705
C_4	0	0	0	0	0	0	0
R^2	0.871	0.913	0.892	0.897	0.925	0.944	0.868
> 4.5 ft and ≤ 7 ft joint spacing	Zone 1	Zone 2	Zone 3	Zone 4	Zone 5	Zone 6	Zone 7
C_1	-0.2169	-0.3455	-0.4058	-0.3747	-0.4566	-0.4726	-0.4968
C_2	1.05296	1.1836	1.2773	1.2575	1.4604	1.5751	1.4385
C_3	0.00581	0.00801	0.00434	-0.000016	-0.007	-0.0129	-0.0025
C_4	0.008295	0.0145	0.01658	0.01371	0.00202	-0.0107	0.00429
R^2	0.857	0.798	0.881	0.870	0.912	0.940	0.862
> 7 ft transverse joint spacing	Zone 1	Zone 2	Zone 3	Zone 4	Zone 5	Zone 6	Zone 7
C_1	0.09321	0.02420	0.11736	-0.0688	-0.2431	-0.0635	-0.0950
C_2	0.76515	0.85253	0.71162	0.92720	1.0960	0.8516	0.9290
C_3	0.01936	0.025210	0.02728	0.02867	0.02822	0.02641	0.02136
C_4	0	0	0	0	0	0	0
R^2	0.659	0.641	0.563	0.615	0.613	0.652	0.683

All adjustment factors are presented with regard to the reference month, January, thus the adjustment factor for January is always one. Therefore, only the monthly HMA modulus for the reference month needs to be determined in order to calculate the remaining HMA modulus values by multiplying the regression equations by the 12 adjustment factors from Equation (15) and Table 4 to give effective HMA modulus values for every calendar month. Regressions were developed for the three different design methods for all 7 AMDAT zones for a total of 21 regressions. The reference month HMA Modulus was found to be a function of the reference

month mid-depth HMA temperature, the HMA thickness, and the project latitude, longitude, and elevation. The reference month mid-depth HMA temperature data was taken from the EICM data. The developed regression models are summarized below with all coefficients and R^2 values for both methods and all seven zones in Equations (16) and Table 5.

$$E_{HMA(Ref)} = C_1 + C_2 * T_{Mid-Depth(Ref)} + C_3 * h_{HMA} + C_4 * Latitude + C_5 * Longitude + C_6 * Elevation \quad (16)$$

where,

$E_{HMA(Ref)}$ is the reference month HMA Modulus,

$T_{Mid-Depth(Ref)}$ is the reference month mid-depth HMA temperature,

h_{HMA} is the HMA thickness, in

$Latitude$ is the geographical latitude of the project location, degrees

$Longitude$ is the geographical longitude of the project location, degrees

$Elevation$ is the distance of the project location above sea level, feet

Table 5: Reference month HMA modulus coefficients by zone

≤ 4.5 ft × 4.5 ft joint spacing	C1	C2	C3	C4	C5	C6	R^2
Zone 1	6902212	-58060.5	-36684	-48511	-3980.3	-9.91	0.901
Zone 2	5746174	-48590	-45205	-32771	505.3	-31.81	0.687
Zone 3	3919812	-20078.4	-45233	17658	-12374.7	52.25	0.654
Zone 4	3951615	-52629	-46317	25747	-2356	17.61	0.859
Zone 5	6172028	-62418	-69110	-31747	1793.9	4.801	0.908
Zone 6	5657489	-48939	-52613	-11091	-7769	-4.95	0.911
Zone 7	4050512	-39010	-56927	35689	-10707	88.486	0.856

> 4.5 ft and ≤ 7 ft joint spacing	C1	C2	C3	C4	C5	C6	R^2
Zone 1	516844	-35706	-65351	-22220	-6306	30.121	0.623
Zone 2	5396644	-40139	-89164	-32803	4454	-45.742	0.558
Zone 3	333077	-26639	-73246	30958	-7350	64.1	0.546
Zone 4	3458108	-35086	-31812	20508	-1956	47.1	0.590
Zone 5	3849527	-45022	-3932	2710	1245	48.4	0.723
Zone 6	3912042	-40680	-8978	-12689	3328	25.1	0.798

Zone 7	3901375	-44662	-10529	36735	-7709	15.89	0.824

> 7 ft transverse joint spacing	C1	C2	C3	C4	C5	C6	R^2
Zone 1	2491478	-10560	-142588	-11145	1813.8	-0.423	0.681
Zone 2	2076287	-6963	-146622	-198	596.9	4.914	0.711
Zone 3	2173722	-586.2	-145128	-4937	-381.7	3.028	0.706
Zone 4	2058023	-1519	-137632	99	-1295.7	5.391	0.685
Zone 5	2174744	-6379	-123582	-3127	69.6	-0.576	0.627
Zone 6	1718085	-2601	-107895	-3189	1959	-9.12	0.594
Zone 7	1734430	-7589	-112461	7729	1172	-2.32	0.687

3.3 Determination of Inputs for HMA Modulus Adjustment Factors and Reference Month HMA Modulus

The calculation of HMA modulus adjustment factors requires HMA thickness and the normalized mid-depth HMA temperature, which is dependent on the temperature region of the project location, as determined from Figure 4. The reference month HMA Modulus equation requires the HMA thickness and the latitude, longitude, and elevation of the project which are all user inputs. Finally, the reference month mid-depth HMA temperature is contingent on the AMDAT zone, as determined from Figure 4.

3.4 Determination of HMA Modulus

The undamaged HMA dynamic modulus value was first estimated for a reference temperature of 70°F using a master curve (ARA, 2004). This undamaged HMA modulus value was then converted to a damaged HMA modulus to reflect the HMA layer condition.

MEPDG (ARA, 2004) provides the following relationship for the damaged HMA modulus:

$$E^*_{HMA(dam)} = 10^{\delta} + \frac{E^*_{HMA(dam)} - 10^{\delta}}{1 + e^{-0.3+5\times\log(\mathrm{d_{AC}})}} \tag{17}$$

where,

$E^*_{HMA(dam)}$ is the damaged HMA modulus, psi.

δ is a regression parameter and is estimated as 2.84 for the default HMA mixture used in the MEPDG.

E^*_{HMA} is the modulus for the undamaged (new) HMA mixture for a specific reduced time which in this procedure is 0.1s.

d_{AC} is the fatigue damage in the HMA layer.

Using the above relationship and Equation (17), the reduction of HMA modulus can be determined. Figure 6 shows the relationship between HMA fatigue damage factor (d_{AC}) and the corresponding reduction factor for the HMA modulus (ΔE^*).

$$\Delta E^* = \frac{E^*_{HMA} - E^*_{HMA(dam)}}{E^*_{HMA}} \tag{18}$$

where,

ΔE^* is the reduction factor for the HMA modulus.

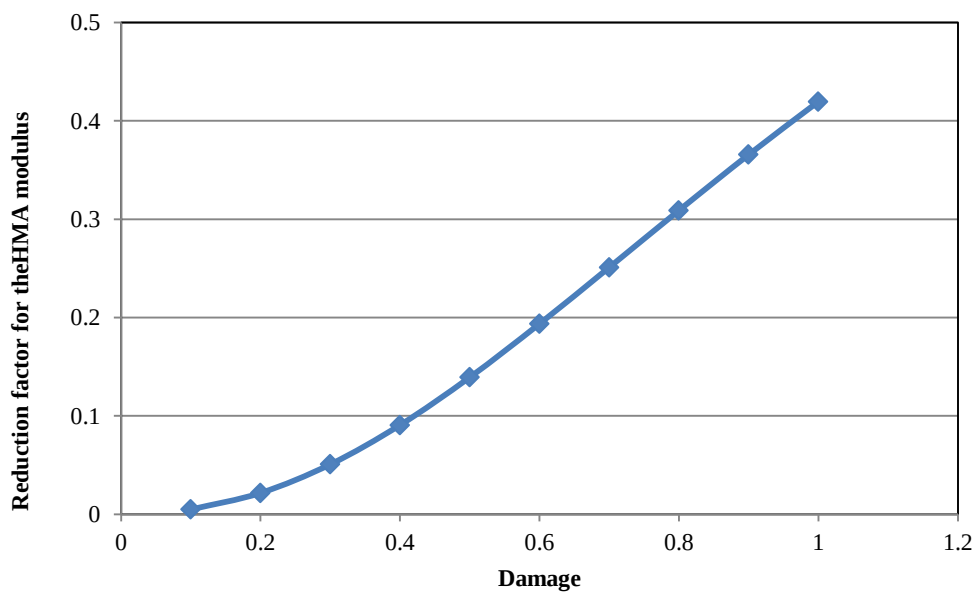

Figure 6: Relationship between the damage in the HMA layer and the corresponding reduction in the HMA modulus.

Next, the HMA damage factor is related to the HMA layer condition. According to the MEPDG (ARA, 2004), the damage factor can be related to the percentage of fatigue cracking as seen in Figure 7. For the application of bonded concrete overlay, Harrington (2008) recommends that fatigue cracking be less than 15% for primary and secondary roadways. In this procedure, the HMA bases for whitetopping are categorized into 'adequate' and 'marginal' based

on their current condition. 'Adequate' HMA conditions represent approximately 0-8% fatigue cracking and a damage factor of 0.3; and 'marginal' HMA conditions represent approximately 8-20% fatigue cracking and a damage factor of 0.4. This is converted to HMA layer condition reduction percentages of 5 and 12.5 percent, respectively, as presented in Table 6.

Table 6: Reduction factor for the HMA modulus.

Existing HMA pavement	Fatigue cracking, %	Damage factor	HMA modulus reduction, %
Adequate	0-8	0.3	5
Marginal	8-20	0.4	12.5

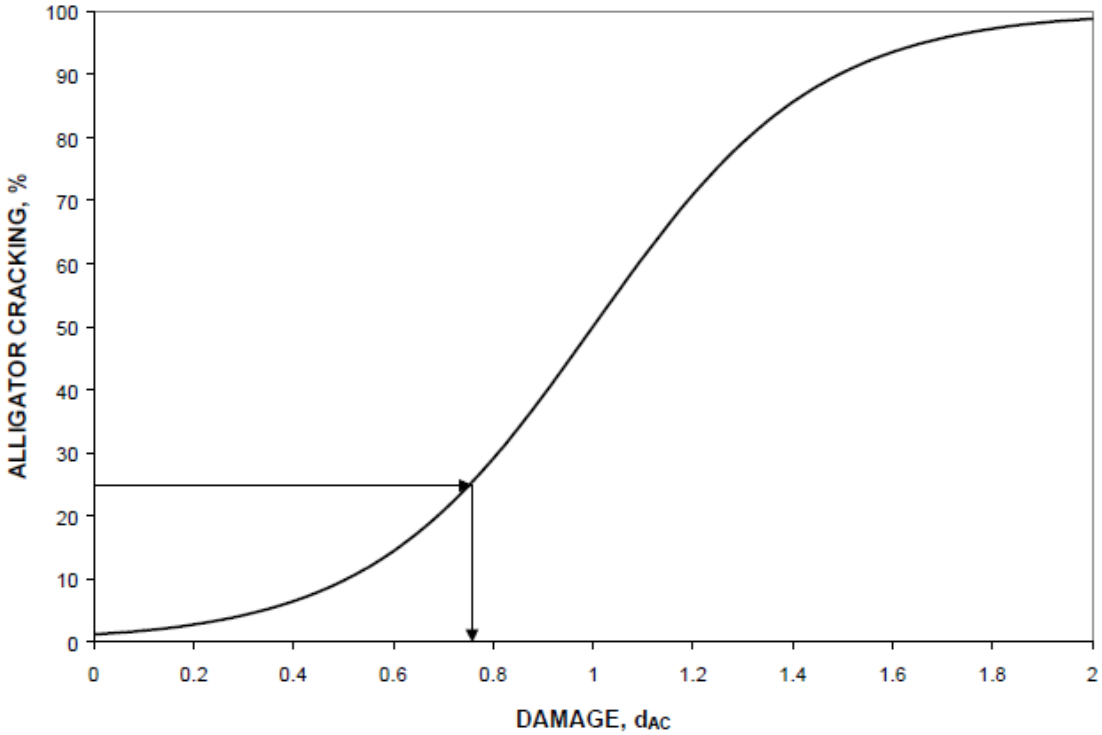

Figure 7: Relationship between alligator/fatigue cracking and damage factor (ARA, 2004).

4. Structural and Fatigue Analysis

The available design procedures specified for whitetopping were developed under the assumption that the failure modes of whitetopping are a function of the PCC thickness; specifically, ultra-thin whitetopping (UTW) failure is governed by corner cracking and thin whitetopping (TWT) failure is governed by transverse cracking. However, a performance review indicates that the actual failure modes are dictated more by slab size than PCC overlay thickness.

Whitetopping projects with a 6 ft × 6 ft joint spacing more frequently experience longitudinal cracking while smaller slabs (such as 3ft × 3ft and 4ft × 4ft) experience corner cracking. This trend can be observed through the distress pattern observed in Minnesota Road Research Facility (MnROAD) whitetopping projects, as shown in Figure 8. A review of the performance of whitetopping sections across the United States supports these conclusions (Li et al 2013). Therefore, different sets of structural equations are used in this design procedure that are for the full lane width, mid-size slabs (greater than 4.5 ft and less than or equal to 7 ft joint square slabs) and smaller slabs (joint spacing less than or equal to 4.5 ft × 4.5 ft), respectively. It is assumed that good jointing practices will be applied and the length to width ratio of the slab will be kept between 1:1 to 1:1.25.

Based on economic considerations, the design thickness in this procedure is limited to 5.5 in for smaller slabs and 6.5 in for larger slabs. For functionality considerations, the recommended minimum PCC thickness is 3.0 in and the minimum HMA layer thickness is also 3.0 in. Additionally, the existing HMA layer thickness is limited to 7 in for the structural and fatigue equations. The benefits of thicker HMA thicknesses diminishes as the HMA thickness becomes increasingly larger than 7 in. The temperature gradient calculations, however, use the given HMA layer thickness and are not limited but provide a limit for the HMA layer stiffness value using similar logic.

(a) Cell 60: 5in; 6ft × 5ft (March 2009)

(b) Cell 63: 4in; 6ft × 5ft (March 2009)

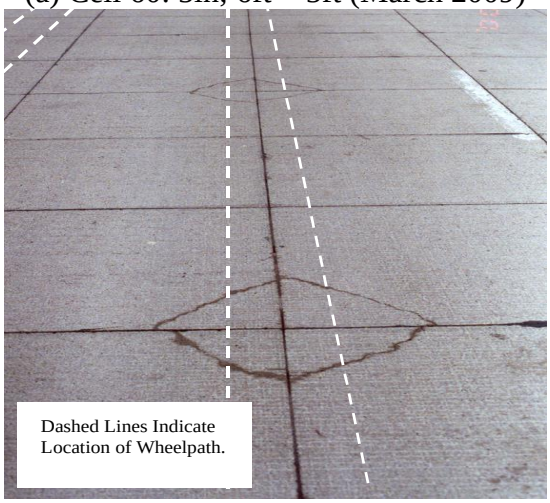

(c) Cell 94: 3in; 4ft × 4ft (2001)

(d) Cell 94: 3in; 4ft × 4ft (2003)

(e) S.H. 119 Test Section No. 2;

Figure 8: Corner, longitudinal and cracking in different slab sizes (Vandenbossche, 2001; Burnham, 2005 and CDOT 2004).

4.1 Design Stress for Slabs Joint Spacing > 4.5 ft and ≤ 7 ft

The predominant failure mode of whitetopping with a 6-ft longitudinal joint spacing was recently identified to be longitudinal cracking in the wheelpath (Li et al 2013). As no structural model was available for this type of distress in existing design procedures, a new structural model was developed to better predict the critical stresses and therefore to provide a more accurate design. A specific 3-D FE model was developed in this study, which was validated by matching the deflections with the FWD data. A database was generated for regression analysis by using a parameter matrix covering the typical ranges of whitetopping structural features.

4.1.1. Mechanical Load-Induced Stress

The critical tensile stress (σ_{18}) in a slab due to an 18-kip ESAL load is given by:

$$\sigma_{Wheel} = \frac{e^{\frac{\left(91.3668 + 0.0512\, h_{HMA}^2 + 8.6096\, h_{PCC}\right) - \log(NA)\left[27.4911 + 7.7478\, h_{PCC} + 7.7478 \log(kE_{HMA})\right]}{15}}}{1.14} + 10 \tag{19}$$

where,

σ_{Wheel} = maximum stress in the PCC overlay under 18-kip wheel load, psi.

h_{HMA} = thickness of the HMA layer, in.

h_{PCC}= thickness of PCC overlay, in.

E_{HMA} = HMA modulus of elasticity, psi.

k = modulus of subgrade reaction, psi/in.

NA = neutral axis from top of PCC overlay, in, which is given in Equation (20).

$$NA = \frac{(E_{PCC} h_{PCC}^2)/2 + \left(E_{HMA} h_{HMA}\right)\left(h_{PCC} + h_{HMA}/2\right)}{E_{PCC} h_{PCC} + E_{HMA} h_{HMA}} \tag{20}$$

where,

E_{PCC} is the PCC elastic modulus, psi and can be estimated from the standard ACI correlation given by:

$$E_{PCC} = 57{,}000\sqrt{f_c'} \tag{21}$$

where,

f'_c is the 28-day compressive strength of the concrete, psi.

4.1.2. Temperature-Induced Stress

The critical temperature-induced stress (σ_T) developed from field measurements by the Colorado Department of Transportation (CDOT) was issued for designing whitetopping projects with a joint spacing greater than 4 ft ×4 ft. Details for the CDOT method of designing whitetopping projects can be found in the work of Sheehan et al. (2004).

The critical temperature-induced stress (σ_T) is described as a percent change in stress from a zero gradient condition and can be calculated as:

$$\sigma_T = 3.85 \times \Delta T \times \sigma_{18} \tag{22}$$

where,

ΔT is the effective equivalent linear temperature gradient (EELTG), °F/in.

4.1.3. Design Stress

The design stress (σ_{Design}) is the sum of the adjusted load- and temperature-induced stresses given by:

$$\sigma_{design} = \sigma_{18} \times F_{stress} + \sigma_T \tag{23}$$

where,

F_{stress} is the stress adjustment factor. The details for the calculation of F_{stress} are presented in Section 4.7.

The performance prediction showed that the model was sensitive to the HMA thickness, especially for extreme values, such as less than 3 in or greater than 8 in. To compensate for this sensitivity, an effective HMA thickness (h^*_{HMA}) is employed in the calculation, as presented in Equation (24). h^*_{HMA} is used in both the structural model and the stress adjustment factor.

$$h^*_{HMA} = (5 \cdot h_{HMA} + 9)/7 \tag{24}$$

4.2. Design Stress for Slabs with Joint Spacing Less than or Equal to 4.5ft × 4.5ft

For joint spacing less than or equal to 4ft × 4ft, the structural equations developed by the by Wu et al. in 1998 to address corner cracks are adopted.

4.2.1. Mechanical Load-Induced Stress

The critical tensile stress (σ_{18}) in a slab due to an 18-kip ESAL load is given by:

$$\log(\sigma_{18}) = 5.025 - 0.465\log(k) + 0.686\log\left({}^{L}/_{l_e}\right) - 1.291\log(l_e) \tag{25}$$

where,

k is the modulus of subgrade reaction, psi/in.

L is the slab length (assuming square slabs), in.

l_e is the effective radius of relative stiffness, in.

h_{HMA} is the HMA thickness after milling, in.

h_{PCC} is the PCC overlay thickness, in.

E_{HMA} is the HMA modulus, psi.

The effective radius of relative stiffness (l_e) for a fully bonded composite pavement is computed using the moment of inertia and the modulus of subgrade reaction as described by:

$$l_e = \left[\frac{(I_m)}{(1 - 0.15^2) \times k}\right]^{0.25} \tag{26}$$

The moment of inertia (I_m) calculation is described by:

$$I_m = \frac{(E_{PCC}h_{PCC}^3)}{12} + E_{PCC}h_{PCC}\left(NA - \frac{(h_{PCC})}{2}\right)^2 + \frac{(E_{HMA}h_{HMA}^3)}{12} + E_{HMA}h_{HMA}\left(h_{PCC} - NA + \frac{(h_{HMA})}{2}\right)^2 \tag{27}$$

where,

The neutral axis (NA) of the composite pavement measured from the top of the concrete layer is described by Equation (20).

4.2.2. Temperature-Induced Stress

The temperature-induced stress (σ_T) is described by:

$$\sigma_T = 28.037 - 3.496(CTE \times \Delta T) - 18.382\,{}^{L}/_{l_e} \tag{28}$$

where,

CTE is the coefficient of thermal expansion, 10^{-6} in/in/°F.

4.2.3. Design Stress

The design stress (σ_{Design}) is the sum of the load- and temperature-induced stresses, as shown in Equation (23).

4.3 Design Stress for Slabs Full Lane Width

The performance data from MnROAD and CDOT indicated that the longitudinal cracking at mid-panel occurred shortly after the 12-ft PCC overlay was constructed but was not followed by additional longitudinal cracking. Unlike the longitudinal cracking in 6-ft slabs, longitudinal cracking in 12-ft slabs are typically located at the mid-slab and not in the wheelpath. The riding quality of the pavement is rarely affected by the mid-slab longitudinal crack and continued deterioration tends not to occur since they are not in the wheelpath. Therefore, the primary mode of failure considered in this design for these slab sizes is transverse cracking.

The structural equations developed for the Colorado Department of Transportation (CDOT) by Sheehan et al. (2004) are adopted here to account for the development of transverse cracking in the larger slab sizes that are a full lane width wide.

4.3.1. Mechanical Load-Induced Stress

The critical tensile stress (σ_{18}) in a slab due to an 18-kip ESAL load is given by:

$$\sigma_{18} = \left[18.879 + 2.918\, {h_{PCC}}/{h_{HMA}} + {425.44}/{l_e} - 6.955 \times 10^{-6} E_{HMA} - 9.0366 \log(k) + 0.0133L \right]^2 \times \frac{18}{20} \tag{29}$$

where,

σ_{18} = maximum stress in the PCC overlay under 18-kip wheel load, psi.

NA = neutral axis from top of PCC overlay, in, which is given in Equation (18).

k is the modulus of subgrade reaction, psi/in.

L is the slab length (assuming square slabs), in.

h_{HMA} is the HMA thickness after milling, in.

h_{PCC} is the PCC overlay thickness, in.

E_{HMA} is the HMA modulus, psi.

l_e is the effective radius of relative stiffness, in.

The effective radius of relative stiffness (l_e) for a fully bonded composite pavement is described by

$$l_e = \left\{ \frac{E_{PCC} \times \left[\frac{h_{PCC}^3}{12} + h_{PCC} \times \left(NA - \frac{h_{PCC}}{2} \right)^2 \right]}{(1 - \mu_{PCC}^2) \times k} + \frac{E_{HMA} \times \left[\frac{h_{HMA}^3}{12} + h_{HMA} \times \left(h_{PCC} - NA + \frac{h_{HMA}}{2} \right)^2 \right]}{(1 - \mu_{HMA}^2) \times k} \right\}^{0.25} \tag{30}$$

where,

μ_{PCC}^2 is the Poisons ratio for the PCC.

4.3.2. Temperature-Induced Stress

The critical temperature-induced stress (σ_T) at the same critical location as the load-induced stress is described as a percent change in stress from zero gradient that can be calculated as:

$$\sigma_T = (3.85 \times \Delta T)\% \times \sigma_{18} \tag{31}$$

where,

ΔT is the effective equivalent linear temperature gradient (EELTG), °F/in.

4.3.3. Design Stress

The design stress (σ_{Design}) is the sum of the load- and temperature-induced stresses, as shown in Equation (23).

The design stress (σ_{Design}) is the sum of the adjusted load- and temperature-induced stresses given by:

$$\sigma_{design} = \sigma_{18} \times F_{stress} + \sigma_T \tag{32}$$

where,

F_{stress} is the stress adjustment factor. As there is no performance data available, the stress adjustment factor, 1.51, developed by CDOT is used.

4.4 Allowable Fatigue Using the PCC Fatigue Equation

The fatigue equation developed by Riley et al. (2005) is used to determine the amount of allowable load repetitions, N_f, as described by:

$$\log(N_f) = \left[\frac{-SR^{-10.24}\log(R)}{0.0112}\right]^{0.217} \tag{33}$$

where,

SR is the stress ratio as defined in Equation (34).

R is the effective reliability taken as 85% in this procedure.

$$SR = \frac{\sigma_{Design}}{\left(1 + R_{150}^{150}\right) \times M_R} \tag{34}$$

where,

R_{150}^{150} is the residual strength ratio characterizing the contribution of the fiber-reinforcement in concrete mixes. The details for the calculation of $R_{150}^{150}$are presented in Section 4.5.

M_R is the modulus of rupture of the PCC overlay, psi and is estimated from the ACI relationship given by:

$$M_R = 2.30{f_c}'^{2/3} \tag{35}$$

where,

$f_c{}'$ is the compressive strength of the PCC, psi

4.5 Fiber Consideration

The use of structural fibers can be considered for whitetopping projects, particularly for PCC overlay thicknesses less than or equal to 4 in. The methodology for accounting for the contribution of fiber, developed by the Illinois Center for Transportation (Roesler et al, 2008), is

adopted in this design. The performance of the whitetopping is enhanced with the inclusion of fiber because of an increased residual strength ratio of the fiber reinforced concrete (FRC). It is hypothesized that the enhanced performance of the FRC whitetopping can be accounted for by adding the residual strength to the modulus of rupture. Therefore, the equivalent stress ratio for the FRC whitetopping can be expressed as Equation (34).

The user can provide the quantity of fiber in terms of weight in pounds per cubic yard of concrete. This information is then used to determine the volumetric quantity of fiber in the mix, which is then used in subsequent calculations.

The absolute volume of fiber is given by:

$$V_{Fiber}^{input} = \frac{W_{Fiber}}{SG \times 62.4 \times 27} \tag{36}$$

where,

V_{Fiber}^{input} is the volume content of the fiber, %.

W_{Fiber} is the weight of the fiber, lb/yd^3.

SG is the specific gravity of the fiber.

The stress factor used throughout this section is the ratio of the enhanced modulus of rupture (considering residual strength) to the original modulus of rupture of the concrete. These stress factors are established based on experimental results. The interpolated stress factors (*ISF*) can be determined by using Equation (37). The *ISF* determines the stress ratio based on the volumetric information of the fiber quantity and maximum and minimum volumes of the recommended fibers and their contributions to the stress factor.

$$ISF = \frac{\left(V_{Fiber}^{input} - V_{MIN}\right)}{\left(V_{MAX} - V_{MIN}\right)}\left(B_{MAX} - B_{MIN}\right) + B_{MIN} \tag{37}$$

where,

V_{MIN} is the minimum absolute volume fraction, %.

V_{MAX} is the maximum absolute volume fraction, %.

B_{MIN} is the minimum stress factor.

B_{MAX} the maximum stress factor.

All four of the above values can be found in Table 7 based on the specific fiber type.

Table 7: Experimentally determined limit values of stress factors for different types of fibers.

Fiber Type	Specific gravity	Absolute volume fraction, %		Stress factor	
		V_{MIN}	V_{MAX}	B_{MIN}	B_{MAX}
None	1.0	100.0	-	1.00	1.00
Synthetic Structural Fibers	0.92	0.194	0.477	1.24	1.39
Steel Fibers	7.80	0.304	0.502	1.10	1.46
Low Modulus Synthetic	0.92	0.097	0.194	1.00	1.05

The minimum and maximum possible absolute weight fractions are computed based on practical recommendations and are provided in Table 8.

Table 8: Recommended fiber content ranges.

Fiber type	Recommended fiber content range (lb/yd^3)	
	$W_{f,MIN}$	$W_{f,MAX}$
Synthetic Structural Fibers	3	7.4
Steel Fibers	40	66
Low Modulus Synthetic	1.5	3

The trial safety factor (SF^{Trial}) is the initial estimate for an equivalent stress ratio factor for a specific fiber type and is given by Equation (38). This consideration accounts for a safety factor in the stress factor:

$$SF^{Trial} = ISF - SF^{0}_{Fiber} \tag{38}$$

where,

SF^{0}_{Fiber} is an arbitrary safety factor of 0.05.

The maximum and minimum allowed factors are then checked using the following equations:

$$SF_{MIN} = \begin{cases} 1.0 & V_{Fiber}^{input} < V_{MIN} \\ SF^{Trial} & V_{Fiber}^{input} \geq V_{MIN} \end{cases} \tag{39}$$

$$SF_{MAX} = \min\left(SF^{Trial}, B_{MAX}\right) \tag{40}$$

The equivalent stress ratio factor (SF^{Final}) is determined by:

$$SF^{Final} = \max\left[1.0, \min\left(SF^{Trial}, B_{MAX}\right)\right] \tag{41}$$

The residual strength ratio characterizing the contribution of the fiber-reinforcement, R_{150}^{150}, is then given by:

$$R_{150}^{150} = SF^{Final} - 1 \tag{42}$$

4.6 Wheel Wander

For whitetopping projects with a 6-ft joint spacing, the critical stresses are located at the bottom of the PCC overlay in the wheelpath. Because wheels wander on the slabs, a fatigue adjustment factor is needed for slabs with a joint spacing greater than 4ft × 4ft to account for the effect of wheel wander ($F_{Wheelwander}$). Finite element modeling (FEM) indicates that the stress distributions at the bottom of the PCC overlay for different load locations match well. Therefore, the normalized stress distribution curve obtained from the case of 4-in PCC placed on top of 6-in HMA was selected to develop $F_{Wheelwander}$. Figure 9 presents the adjustment factors for wheel wander at reliability of 50% and the equation for $F_{Wheelwander}$ is described as

$$F_{Wheelwander} = 2.0405 \times SR^{-1.695} \tag{43}$$

where,

SR is thestress ratio as defined in Equation (34).

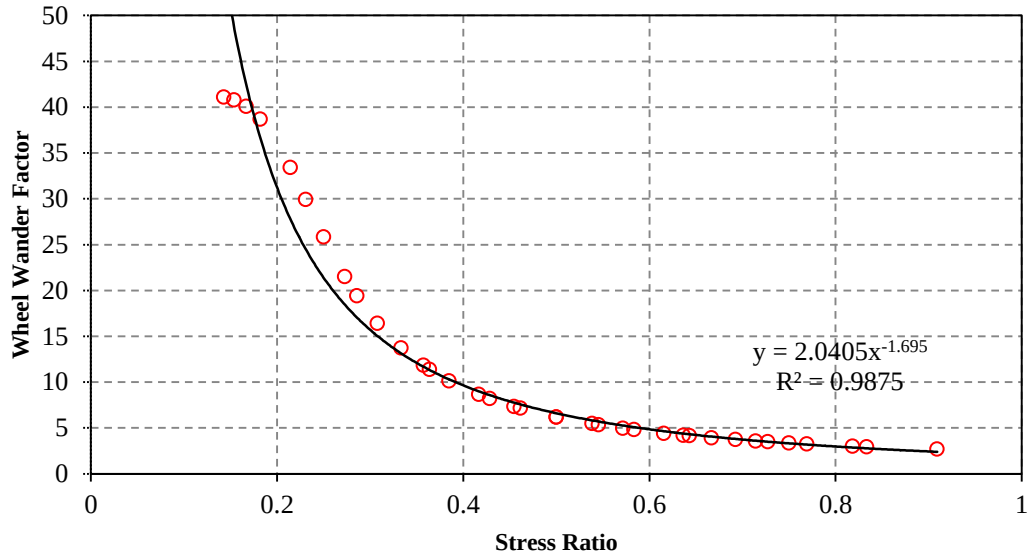

Figure 9: Fatigue adjustment factor for wheel wander in the design for slabs with joint spacing greater than 4ft × 4ft.

4.7 Stress Adjustment Factors

The stress adjustment factors are determined by calibrating the predicted performance in terms of fatigue damage to field distress measurements (percentage of slab cracking) using data from known whitetopping projects. Whitetopping projects listed in Table 9 are incorporated into the calibration database where 100% fatigue damage corresponds to 25% slabs cracked. Figures 10 and 11 show the adjustment factors generated by matching the predicted fatigue damage to the performance data of MnROAD Cells 93, 94, 95, 60 and 62.

The stress adjustment factors obtained for all projects in the database are then statistically correlated to pavement design features and are described by:

F_{stress} for slabs spanning the full lane width:

$$0.205h_{HMA} - 0.0296h_{PCC} + 0.65$$

F_{stress} for a joint spacing greater than 4.5 ft and less than 7 ft:

$$(1.70815412 - 0.03953861 \cdot \min(4, h_{pcc}) + 0.03623689 \cdot h_{HMA} - 0.01942344 \cdot h_{HMA}^2 + 0.00091517 \cdot h_{HMA}^3) \cdot \left(\frac{MOR}{650}\right)^{0.35} \quad (44)$$

F_{stress} for a joint spacing less than or equal to 4.5 ft:

$$10^{\left[0.61073-0.1066\cdot\log(h_{pcc})-0.705\cdot\log\left(h_{HMA}\right)+0.00861\cdot h_{HMA}^{2}\right]}\cdot\left(\frac{650}{MOR}\right)^{0.5} \quad (45)$$

Table 9:Whitetopping projects included in the calibration database for determining the stress adjustment factors.

State	Project	h_{PCC}, in	h_{HMA}, in	Slab size, ft × ft	F_{Stress}
Minnesota	Cell95, MnROAD	3	10	6 × 6	2.20
	Cell62, MnROAD	4	8	6 × 5	2.31
	Cell60, MnROAD	5	7	6 × 5	2.20
	Cell 93, MnROAD	4	9	4 × 4	1.325
	Cell 94, MnROAD	3	10	4 × 4	1.192
Missouri	Intersection of SR 291 and SR 78	4	4	4 × 4	1.37
	US-60 between US 71 and US 71 near Neosho	5	4.5	4 × 4	1.38
New York State	NY-408 and SH-622	4	9.5 (7)	4 × 4	0.77
Illinois	Highway 4- Piatt County	5	4	5.5 × 5.5	2.00
	Highway 2- Cumberland County	5.75	6.5	5.5 × 6	2.00
Colorado	US85- Section1	4.7	4.5	5 × 5	1.55
	US85- Section 2	5.8	5.9	5 × 5	1.80
	US85- Section 3	6	5.4	5 × 5	1.85
	SH 119- Section 1	5.1	3.3	6 × 6	1.60
	SH 119- Section 3	6.3	3.4	6 × 6	1.84
	SH 119- Section 4	7.3	3.4	6 × 6	2.10

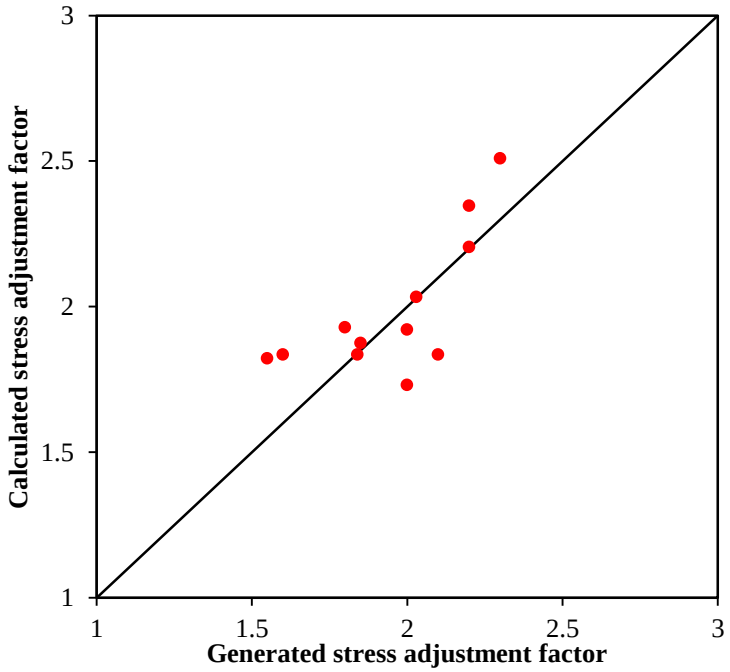

Figure 10: Stress adjustment factors for slabs with joint spacing greater than 4ft × 4ft.

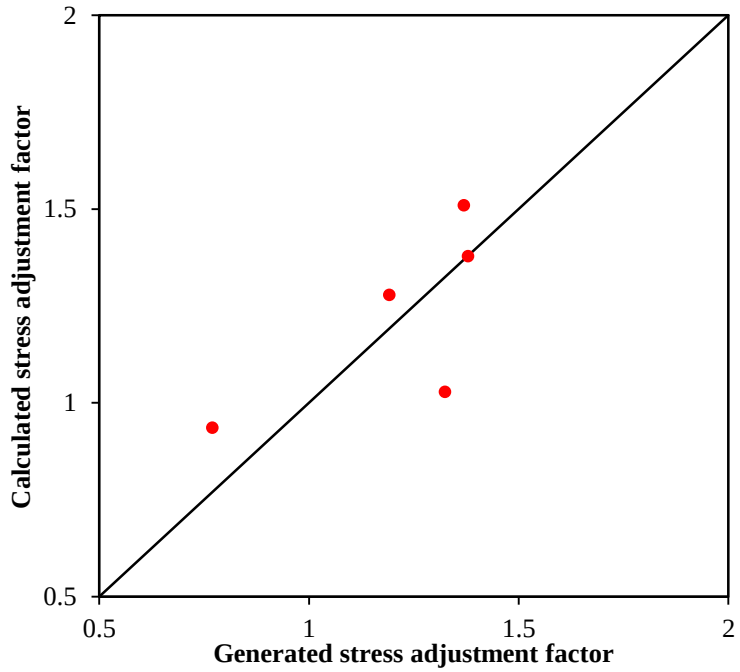

Figure 11: Stress adjustment factors for slabs with a joint spacing less than or equal to 4ft × 4ft.

Figures 12 to 15 present the performance data and the predicted fatigue of Cells 60, 62, 93, 94 and 95, respectively.

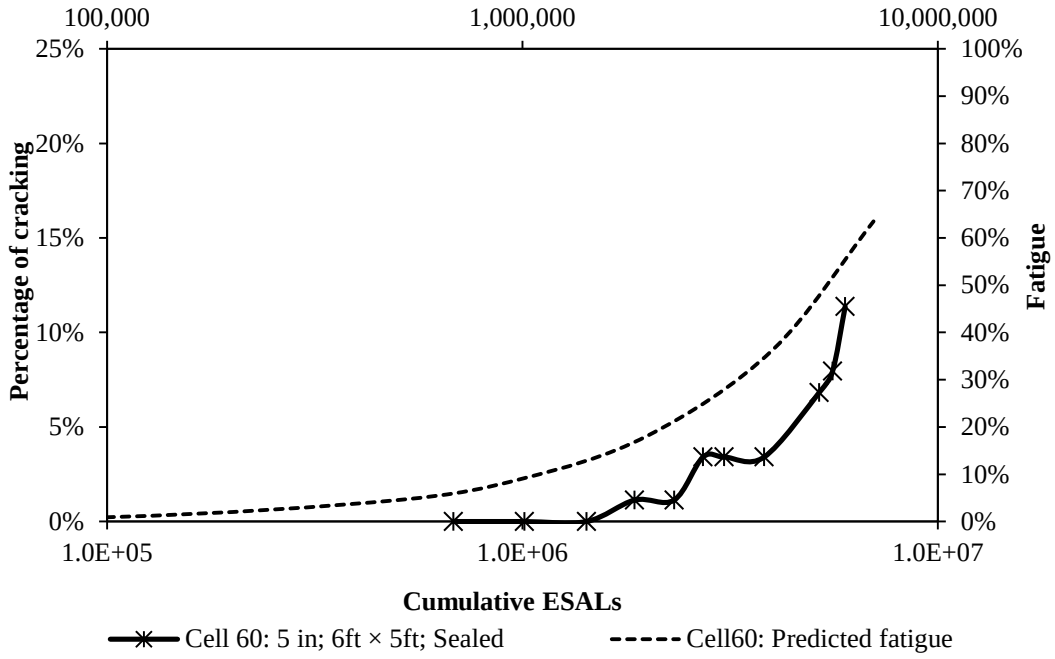

Figure 12: Performance data and predicted fatigue of Cell 60.

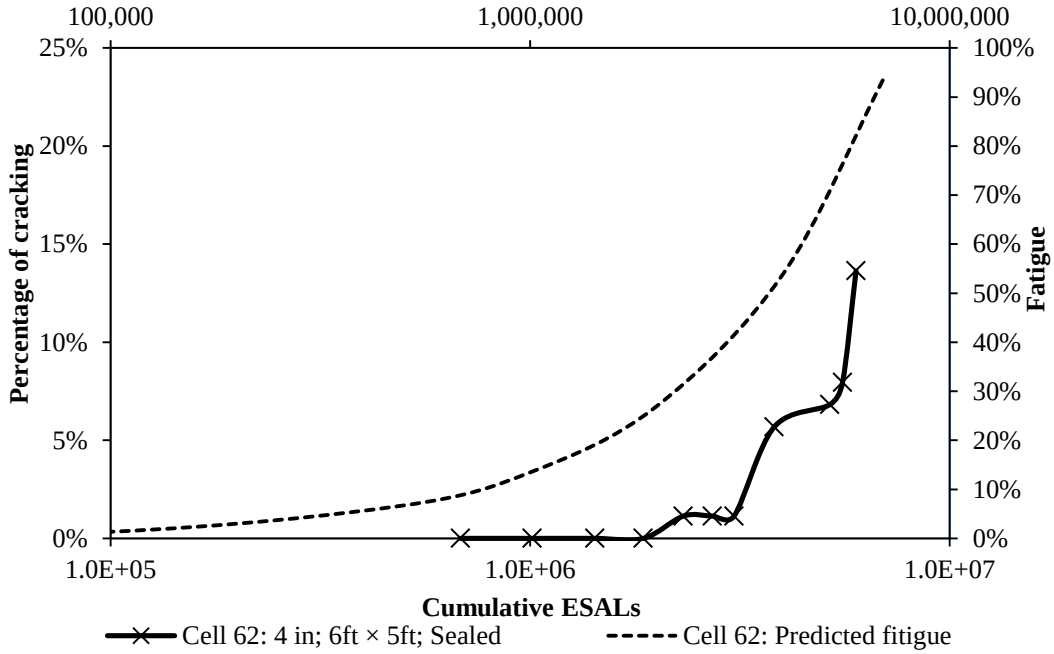

Figure 13: Performance data and predicted fatigue of Cell 62.

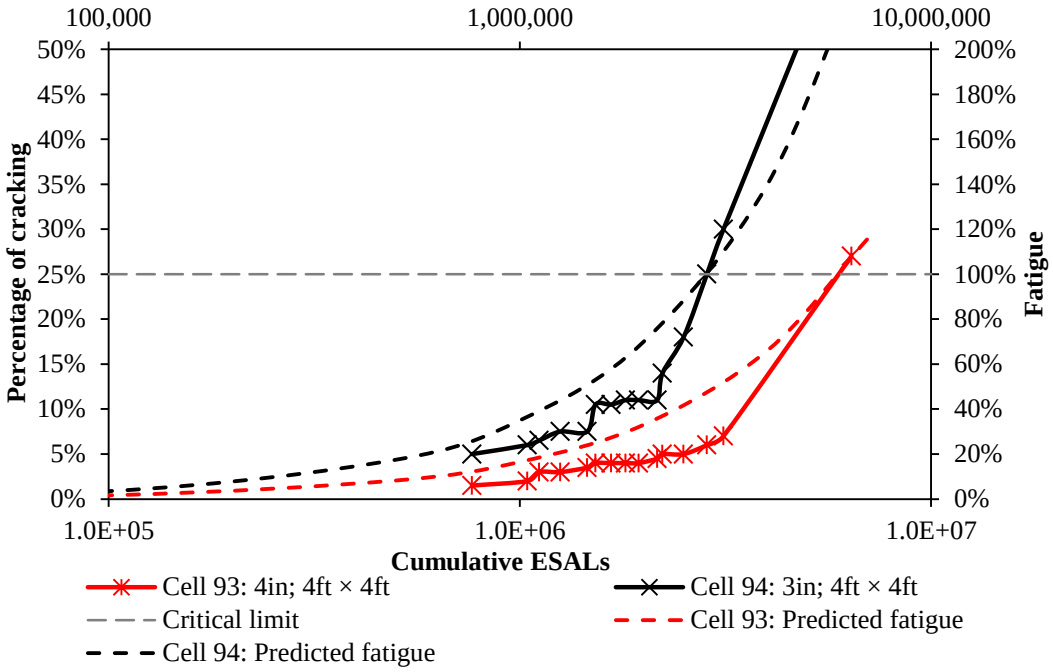

Figure 14: Performance data and predicted fatigue of Cells 93 and 94.

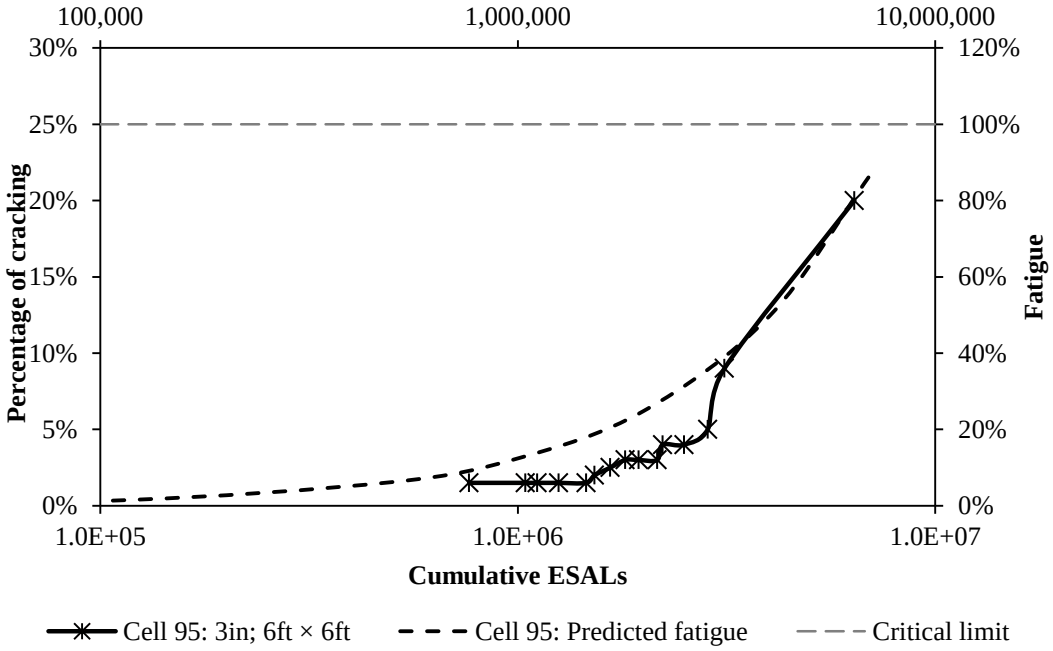

Figure 15: Performance data and predicted fatigue of Cell 95.

4.8 Joint Sealing Effect

Performance data indicates that sealed whitetopping sections perform better than unsealed sections, as shown in Figure 16 (Burnham, 2013). Performance reviews of BCOA

sections at MnROAD indicate that unsealed whitetopping sections would have an increase in PCC design thickness of approximately 0.5 in. This design procedure is developed using the sealed whitetopping design as the standard design.

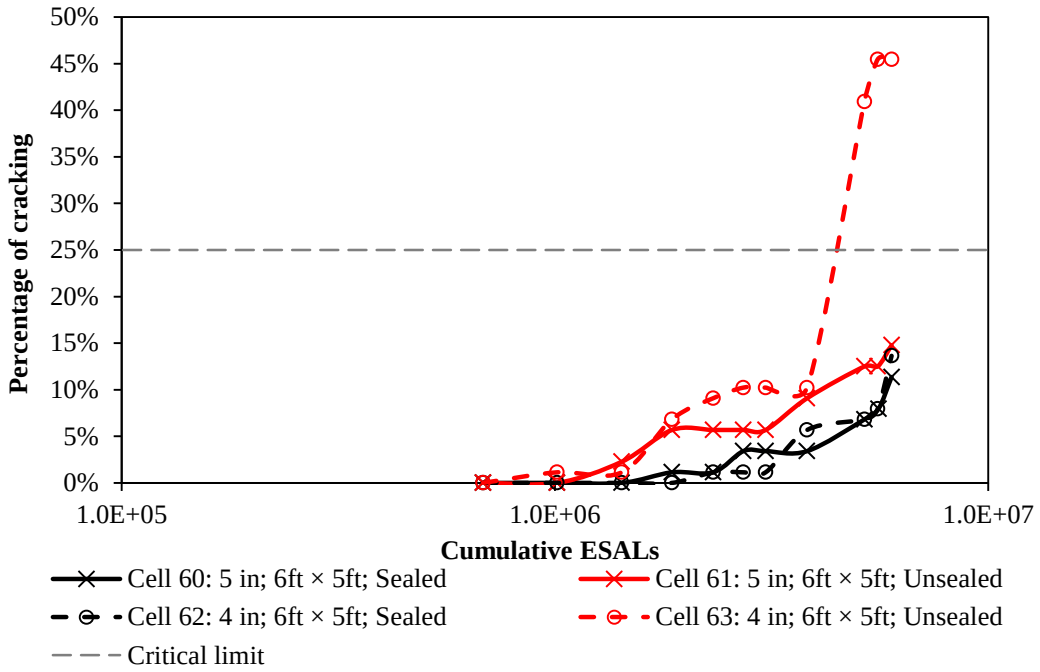

Figure 16: Performance data of sealed and unsealed sections in MnROAD.

5. Conclusion

The BCOA-ME has been developed to provide a tool for predicting the overlay thickness for bonded concrete overlays over distressed HMA or composite pavements for a range of panel sizes. Previous procedures used for designing these structures were limited to the design of either UTW or TWT. This procedure allows the mode of failure to be dictated by the panel size and not the overlay thickness. With the BCOA-ME, the designer has the ability to use one tool for the design of all bonded overlays over HMA.

References

American Concrete Pavement Association (ACPA).*Design of Concrete Pavement for City Streets*. ACPA Publication IS184-P, American Concrete Pavement Association, Skokie, IL, 2002.

American Concrete Pavement Association (ACPA). *Whitetopping—State of the Practice*. ACPA Publication EB210P, American Concrete Pavement Association, Skokie, IL, 1998.

ARA, Inc. *Guide for Mechanistic-Empirical Design of New and Rehabilitated Pavement Structures*. National Cooperative Highway Research Program, Transportation Research Board, National Research Council, Washington, DC, 2004.

Barman, M., F. Mu and J.M. Vandenbossche. *Development of a Rational Mechanistic-Empirical Based Design Guide for Thin and Ultrathin Whitetopping, Task 4: Climatic Considerations*.Federal Highway Administration (FHWA) Pooled Fund study, TPF 5-165, 2011, p 1-71.

Burnham, T. R. *Forensic Investigation Report for Mn/ROAD Ultrathin Whitetopping Test Cells 93, 94 and 95*. Report MN/RC-2005-45, Minnesota Department of Transportation, St. Paul, MN, 2005.

Burnham, T. R. *Construction Report for Mn/ROAD Thin Whitetopping Test Cells 60-63*. Report MN/RC -2006-18, Minnesota Department of Transportation, St. Paul, MN, 2006.

Burnham, T. R. *The Effect of Joint Sealing on the Performance of Thin Whitetopping Sections at MnROAD.* Minnesota Department of Transportation, St. Paul, MN, 2013.

Gucunski, N. *Development of a Design Guide for Ultra Thin Whitetopping (UTW).* Research report. New Jersey Department of Transportation, 1998.

Harrington, D. *Guide to Concrete Overlays: Sustainable Solutions for Resurfacing and Rehabilitating Existing Pavements*. National Concrete Pavement Technology Center, 2008, p. 69.

Larson, G. and B. Dempsey, (2003). *EICM Software*. Enhanced Integrated Climatic Model Version 3.0 (EICM). University of Illinois, Urbana, IL.

Li, Z. and J. M. Vandenbossche, *Redefining the Failure Mode for Thin and Ultra-thin Whitetopping with 1.8-m by 1.8-m (6- x 6-ft) Joint Spcaing*. Transportation Research Record: Journal of Transportation Research Board, Transportation Research Board of the National Academics, Washington, DC, 2013.

Mindess, S., J.F. Young and D. Darwin. "Concrete: Second Edition". Pearson Education, Inc., 2003, p. 312-217.

NOAA Satellite and Information Service. (2010a). "Annual mean daily average temperature." National Environmental Satellite, Data, and Information Service. <http://cdo.ncdc.noaa.gov/climaps/temp0313> (Jan. 10, 2010).

National Renewable Energy Laboratory (2009) "Annual Concentrating Solar Resource Map" National Renewable Energy Laboratory. <http://www.nrel.gov/gis/solar.html>(May 2010).

Pavement Systems LLC. (2005). *LTTPBIND Version 3.1*,a Superpave Binder selection program, developed by Pavement Systems LLC for Federal Highway Administration Asphalt Team – HTA-23. Bethesda, MD.

Rasmussen, R.O. and D.K.Rozycki. *Thin and Ultra-Thin Whitetopping*. NCHRP Synthesis of Highway Practice 338, National Cooperative Highway Research Program, National Research Council, Washington, DC, 2004.

Riley, R.C., L. Titus-Glover, J. Mallela, S. Waalkes, and M. Darter. *Incorporation of Probabilistic Concepts into Fatigue Analysis of Ultrathin Whitetopping as Developed for the American Concrete Pavement Association*. Proceedings from the Best Practices in Ultra Thin and Thin Whitetopping, Denver, Colorado, April 12-15, 2005, p. 288-317.

Roesler, J., A. Bordelon, A. Ioannides, and M. Beyer. *Design and Concrete Material Requirements for Ultra-Thin Whitetopping*. Illinois Center for Transportation, Report No. FHWA-ICT-08-016, 2008, p E1-E26.

Sheehan, M.J., S.M. Tarr, and S. Tayabji. *Instrumentation and Field Testing of Thin Whitetopping Pavement in Colorado and Revision of the Existing Colorado Thin Whitetopping Procedure*. Colorado Department of Transportation Research Branch. Report No. CDOT-DTD-R-2004-12, 2004.

Vandenbossche, J.M. *Performance Analysis of Ultrathin Whitetopping Intersections on US-169, Elk River, Minnesota*. Transportation Research Record: Journal of the Transportation Research Board, No. 1853, Transportation Research Board of the National Academics, Washington, DC, 2003, pp. 18-27.

Vandenbossche, J. M. and A. J. Fagerness. *Performance, Analysis, and Repair of Ultrathin and Thin Whitetopping at Minnesota Road Research Facility*. Transportation Research Record: Journal of Transportation Research Board, No. 1809, Transportation Research Board of the National Academics, Washington, DC, 2002, pp. 191-198.

Wu, C.L., S.M. Tarr, T.M. Refai, M.A. Nagai, and M.J. Sheehan. *Development of Ultra-Thin Whitetopping Design Procedure.*Report RD 2124. Portland Cement Association, Skokie, IL, 1998.